

# Photo excited scanning probe microscopy for buried nano structure analyses

M. Ishii, K. Sakurai, N. R. J. Poolton\* and B. Hamilton\*\*

National Institute for Materials Science (NIMS), 1-2-1 Sengen, Tsukuba, Ibaraki, 305-0047

Fax: 81-29-860-4706, e-mail: ISHII.Masashi@nims.go.jp

\*Daresbury Laboratory, Warrington WA4 4AD, UK

\*\*University of Manchester, P.O. Box 88, Manchester M60 1QD, UK

For buried nano structure analyses, we combined a scanning probe microscope with either a UV laser or x-ray light source. Electron trapping process at Si/SiO<sub>x</sub> buried interface under UV laser irradiation was investigated with an electrostatic force microscope (EFM). The EFM signal synchronized with optical shutter operation revealed electron trapping process with the time constant of 33 ~ 87 s dependent on laser power. These large values reveal a quasi-stable photoionization state of the trapping site. The EFM with the x-ray source provided an x-ray absorption spectrum of the electron trapping site. The inner-shell excitation and following relaxation of trapped electron into the core-hole result in the quasi-stable photoionization state. Since the photoionization can be detected with EFM easily, nano x-ray absorption spectra can be probed with high efficiency. The trapping site had deeper inner-shell energy level owing to electric field between the sample surface and probing tip, resulting in an energy shift of the absorption spectrum. An estimation of electric field due to the trapped electron reproduced the energy shift. The electric field was dominantly determined by a trapped electron in the nanometer area under the tip, and indicated potential for nano spectroscopy of EFM with an x-ray source.

Key words: UV, X-ray, Electrostatic Force Microscopy, photoionization, x-ray absorption spectra

## 1. INTRODUCTION

Scanning probe microscopy (SPM) has been widely used for observation of surface with atomic resolution. Surface topography and various physical properties such as electric potential [1,2] and magnetic orientation [3] of nanometer domains can be evaluated with SPM systems. On the other hand, chemical properties such as elements distribution and bonding states of elements cannot be dealt with by using any SPM system without difficulty. To deal with chemical properties by using SPM, we have tried to combine an SPM system with light sources, such as an ultra violet (UV) laser [4] or an x-ray light source [5,6].

It is important to note that the SPM combined with light source would be another breakthrough in SPM technique, i.e., buried structure observations. The UV and x-ray lights penetrate into the sample, indicating that buried structures can be excited by the lights and the SPM can detect the signals from the buried nano structures.

In this work, we used electrostatic force microscopy (EFM) [7] as SPM. Since the EFM is sensitive to localized charges, we could selectively evaluate electron trapping sites below the surface. The electron trapping sites determine properties of a material, such as electric conductivity, chemical reaction, etc. Obviously, the electron trapping sites are landmarks in material research. Therefore, we adopted EFM with a light source to chemical analyses of an electron trapping site. In the following discussion, EFMs under UV or x-ray irradiation are denoted as UV-EFM and X-EFM, respectively.

## 2. EXPERIMENTS

The experiments were performed with custom made

non-contact AFM/EFM system (UNISOKU Co. Ltd.). Figure 1 is schematic diagram of the system. For convenient of light irradiation, the sample was vertically mounted on a scanning stage opposite to a piezoelectric cantilever. The cantilever made from lead zirconate titanate (PZT) was used for actuating and sensing along the z-axis of a probe tip [8]. The cantilever was resonantly oscillated at an eigenfrequency (About 110 kHz) by the PZT actuator. The piezoelectric cantilever is more appropriate than an optically monitored cantilever for the photo-excitation experiment since the light for the optical cantilever might induce undesirable surface excitation.

We detected local charge by using a lock-in amplification technique with modulation bias voltage  $V_b$  applied to the sample stage. The probe tip was coated with a metal film of the Cr (5 nm)/Au (20 nm) for electric conduction, and connected to the ground. The modulation frequency and amplitude of  $V_b$  were 3 - 10 kHz and 2 V, respectively. The probe head was installed into a vacuum chamber to avoid air absorption of soft x rays in X-EFM experiments.

UV photons or x rays are introduced into the sample with the incident angle of  $\sim 54^\circ$  from the perpendicular to the surface. The light directly irradiates the spot under the probe. The light source for UV-EFM was a He-Cd laser (Kimmon Electric Co., LTD., IK5552R-F with the maximum power of 25 mW for  $\lambda = 325$  nm). In UV-EFM experiments, we observed time transition signal by using an optical shutter synchronized by a computer system with the UV-EFM signal collection. On the other hand, the light source for X-EFM was the beamline MPW 6.1 at the Daresbury synchrotron facility in the UK [9]. The MPW 6.1 has a multi-pole wiggler as an insertion device that provides tunable x rays within a

photon energy range of 40-400 eV. The x rays were monochromatized by grating installed in the beamline. The x-ray absorption spectra were obtained with photon energy scanning by changing the grating angle.

The sample used in this study was a (111)-oriented n-type Si wafer. Its resistivity was 38 - 55  $\Omega\cdot\text{cm}$ . The sample was introduced into the EFM system without any chemical treatment. Therefore, the Si surface was covered with a native oxide of nanometer thickness. Though we investigated an as-prepared wafer in this study, we also confirmed by scanning tunneling microscopy that this sample had a clean, flat surface with the well-known  $7 \times 7$  reconstruction after thermal treatment in a vacuum.

Nanometer thick oxide films are used as a gate insulator in recent nano-scale Si transistors. Since a single electron trapping site in the insulator degrades device performance, chemical analyses of the trapping site are required. The sample is appropriate for the demonstration of UV- and X-EFM.

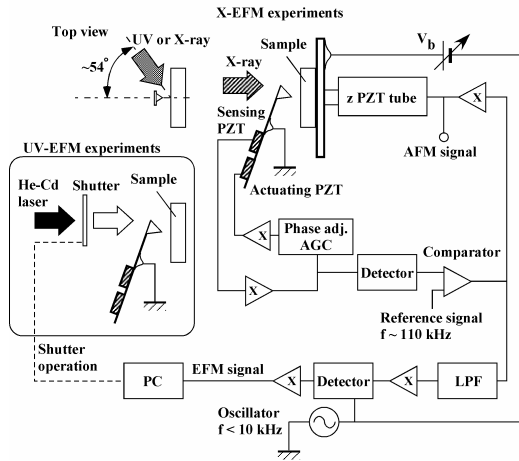


Fig. 1 Non contact AFM/EFM system used in this study. UV laser beam or x-ray beam can be introduced into the system. In UV-EFM experiments, time transition signal was observed using an optical shutter synchronized with the UV-EFM signal collection. In X-EFM experiments, beamline MPW 6.1 of synchrotron radiation source (SRS) in UK was used as the x-ray source.

### 3. RESULTS AND DISCUSSION

#### 3.1 UV-EFM

The inset of figure 2 shows UV-EFM signal  $I_{UV-EFM}$  with respect to time  $t$  after the laser was on. The laser power  $P_w$  was fixed at 1.42 mW, and  $V_b$  was -4 V. As shown in this figure, the UV-EFM signal increases gradually after the laser is turned on, and finally saturated. This slow time transition suggests that the sample has an electron trapping site, and it corresponds to the trapping process of electrons induced by UV light. This result does not identify the vertical position of the trapping sites. However, the negative  $V_b$  inducing electron accumulation at the Si oxide / Si wafer interface was favorable to obtain the conventional EFM images [4], indicating that the electron trapping sites are located

at the buried interface.

Based on a model assuming that electron trapping probability is proportional to the density of unoccupied trapping sites, a rate equation analysis can be demonstrated [10]. The analytical solution of the rate equation gives  $I_{UV-EFM}$  dependent on  $t$  as

$$I_{UV-EFM} = A(1 - \exp(-t/\tau)) + B \quad (1),$$

where  $A$  and  $B$  are the constant. In fact, as shown by solid line in the inset of figure 2, Eq. (1) reproduces the experimental result. In this equation,  $\tau$  is a time constant dependent on  $P_w$ . From the similar time transition experiments for  $P_w$  of 0.5 and 1.1 mW,  $\tau^{-1}$  dependent on  $P_w$  can be obtained as shown in figure 2. From this figure, one can see that  $\tau^{-1}$  is directly proportional to  $P_w$ , i.e.,  $\tau^{-1} = 0.0212 P_w$ . From the fact that the number of photo induced electron is proportional to  $P_w$ , this finding indicates the trapping process is limited by the number of free electrons in the sample.

On the other hand,  $\tau^{-1}$  from 0.0115 to 0.0300  $s^{-1}$  ( $\tau = 33 \sim 87$  s) indicates the trapping process is slow. The electron dynamics with time scale  $> 30$ s are reported for various oxides which have trapping sites with deep energy level [11,12]. The trapping sites at the build interface found in this study would have a deep energy level.

The liner  $P_w$  dependence and slow  $\tau$  values denote the quasi-stable state of the valence hole at the trapping sites in this system. The quasi-stability is a key factor for sensitive signal detection in following X-EFM measurements.

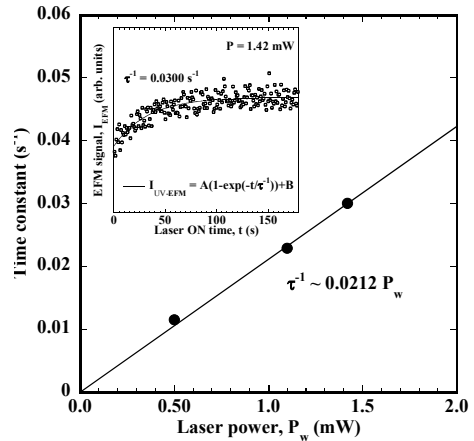


Fig. 2 The inverse time constant  $\tau^{-1}$  with respect to laser power  $P_w$ . The inset shows UV-EFM signal  $I_{UV-EFM}$  with respect to time  $t$  after laser on.  $\tau^{-1}$  was estimated from the fitting of  $I_{UV-EFM}$  by using Eq. (1).

#### 3.2 X-EFM

Figure 3(a) indicates X-EFM signal with respect to photon energy, i.e., the X-EFM spectrum. The photon energy around 100 eV is for tuning to the Si  $L$  absorption edge. In this experiment,  $V_b$  was fixed at 0 V. As shown in this figure, the edge jump at 107.1 eV and following absorption peaks denoted by P1, P2, and P3 were observed. Since X-EFM reveals an electron trapping site under the probe, this figure indicates the

x-ray absorption spectrum of the electron trapping site.

As a reference, an x-ray absorption spectrum obtained with a conventional method probing total electron yield (TEY) is shown in figure 3(b).

This TEY from the whole x-ray irradiation area indicates the x-ray absorption spectrum of major Si atoms without an electron trapping level. Obviously, the major Si atoms form SiO<sub>2</sub>. As shown in this figure, the edge jump at 104.5eV and following peaks are revealed. A comparison between figures 3(a) and (b) reveals that the edge jump of X-EFM is shifted to higher energy by 2.6 eV. The edge jump shift to higher energy cannot be explained as a chemical shift owing to SiO<sub>x</sub> (x<2). In general, SiO<sub>x</sub> (x<2) indicates the edge jump shift to lower energy in the x-ray absorption spectrum.

For more detailed consideration of the edge jump shift observed in figure 3, we introduce a model in which potential well of Si 2p state  $\Delta V_{2p}$  is induced by electric field owing to a trapped electron. Since  $\Delta V_{2p}$  is deepen the Si 2p state, we need higher excitation energy by  $\Delta V_{2p}$ . Hence,  $\Delta V_{2p}$  can be evaluated from the edge jump shift in x-ray absorption spectrum.

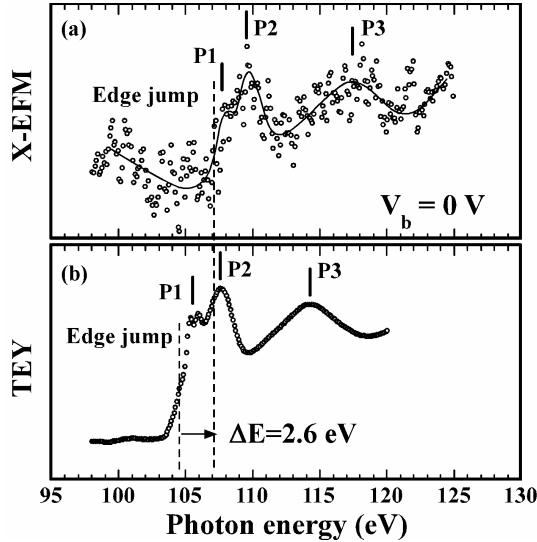


Fig. 3 (a) X-EFM spectrum at Si L-edge. (b) X-ray absorption spectrum evaluated by a conventional method of probing total electron yield (TEY)

The inset of figure 4 is a cone model used for electric field calculation. As shown in this figure a virtual charge-ring with  $\delta a$  width on the sample surface induces partial electric field  $dE$  at  $z$ . Here,  $z$  is the distance between the X-EFM probe and the sample surface,  $a$  is the radius of the base of the cone, and  $\lambda$  is the trapped electron density. The partial electric field perpendicular to the sample surface,  $dE \cos \theta$ , can be calculated from this cone model:

$$dE \cos \theta = \frac{\lambda z a}{2\epsilon_0 (a^2 + z^2)^{3/2}} \quad (2),$$

where  $\epsilon_0$  is the dielectric constant of the vacuum. The definite integration of Eq. (2) over the sample

surface ( $0 < \theta < \pi/2$ ) gives the total electric field  $E_{total}$  at the probe tip; thus  $E_{total} = \lambda/2\epsilon_0$ . This result indicates that  $E_{total}$  is constant for given  $\lambda$ . In the X-EFM experiment, since the  $V_b = 0$  V,  $E_{total}$  should be balanced with  $\Delta V_{2p}$ . This balance can be expressed as

$$\Delta V_{2p}/z = \lambda/2\epsilon_0. \quad (3)$$

Therefore,  $\lambda$  can be estimated to be  $2\epsilon_0 \Delta V_{2p}/z$ . On the other hand, we experimentally obtained  $\Delta V_{2p}$  of 2.6 eV as shown in figure 3. The typical  $z$  in SPM is a few nm. The substitution of  $\Delta V_{2p}/z \sim 1 \times 10^9$  V/m and  $\epsilon_0$  of  $8.854 \times 10^{-12}$  F/m leads to  $\lambda \sim 1.6 \times 10^{-2}$  C/m<sup>2</sup>. Therefore, the density of the trapping site is estimated to be  $\sim 1 \times 10^{17}/m^2 = 1 \times 10^{-1}/nm^2$ . This value indicates the trapping centers are statistically distributed with  $\sim 3$  nm period. This period is consistent with an experimental result obtained with conventional EFM [4].

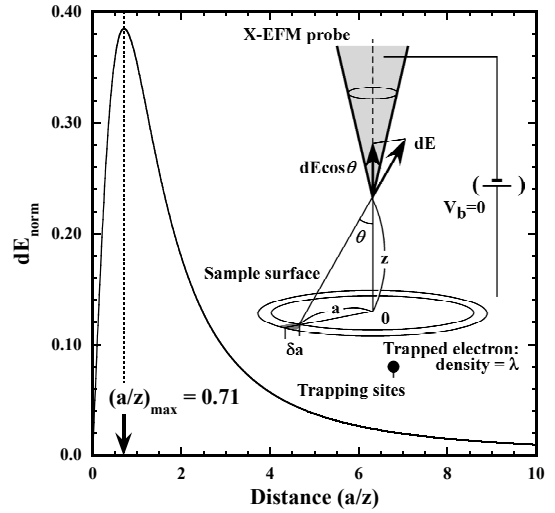


Fig. 4 Normalized partial electric field  $dE_{norm}$  defined as  $dE \cos \theta / E_{total}$  with respect to normalized distance  $z/a$ . For this calculation, the cone model shown as an inset was used.

For this estimation,  $E_{total}$  was derived from definite integral of  $dE \cos \theta$  over  $0 < \theta < \pi/2$ ; infinitely distant trapped electrons were taken into account. This apparently contradicts the nano spectroscopy of X-EFM. However, the following discussion explains that the calculation model affirms the nano scale spatial resolution involved in this method. Figure 4 shows normalized partial electric field  $dE_{norm}$  defined as  $dE \cos \theta / E_{total}$  with respect to normalized distance  $z/a$ . As shown in this figure,  $dE_{norm}$  had a sharp peak, and rapidly decreased with increasing  $z/a$ . Though  $E_{total}$  was calculated with the trapped electrons on the whole surface, this sharp peak indicates that  $E_{total}$  is determined by the trapped electrons under the probe.

In fact, the trapped electrons within  $a/z < 2.77$  provide 2/3 of  $E_{total}$ . Especially, the result that the strong  $dE_{norm}$  peak with the maximum position  $(a/z)_{max} = 0.71$  suggests that X-EFM can distinguish chemical states on the surface with nm spatial resolution. This consideration is consistent with the demonstration of a

chemical state mapping as one of applications of X-EFM [6].

In X-EFM spectroscopy of buried nano structures, the quasi-stable state of the valence hole as discussed in UV-EFM plays an important role. X-EFM spectra can be obtained with x-ray induced photoionization of the electron trapping sites. In other words, the inner-shell excitation with electron emission and following relaxation of trapped electrons into the core hole results in the quasi-stable state of the valence hole. Generally speaking, the core hole has extremely short lifetime of  $\sim$ fs. The photoionization yielding the quasi-stable state is equal to the conversion of the fast electron transition process of  $\sim$ fs to the slow process with  $>$  ms. Obviously, the slow electron transition process can be easily detected with EFM. This conversion effect improves the detection efficiency, and provides the nano spectra of the electron trapping sites with low density.

#### 4. SUMMARY

For chemical analyses by using scanning probe microscope, we introduced either a UV laser beam or an x-ray beam into an electrostatic force microscope (EFM). Using the EFM, we selectively observed electron dynamics at Si/Si oxide interface with an electron trapping site. For the UV irradiation experiments, the electron migration in the conduction band was characterized by an electron trapping time constant. The trapping time constant depended on laser power, and we obtained large values from 33 to 87 s.

These long time constants reveal quasi-stable state of the valence hole in this system. For the X-ray irradiation experiments, EFM signal dependent on the photon energy revealed the x-ray absorption spectrum of the trapping site. The edge jump energy of the spectrum was shifted to higher energy by 2.6 eV than that of the conventional x-ray absorption spectrum evaluated from total electron yield. This finding can be explained by the local electric field between probe tip and trapping electron. The electric field makes a tighter binding of the Si  $2p$  electron at the trapping site, so that higher photon energy is necessary for excitation of the electron.

#### Acknowledgements

The Authors would like to acknowledge the support of the EPSRC and of JASRI which made this work possible and to thank Joel Chevrier, Daniel Pialhary and Juris Purans for useful discussions. This work was supported by a Grant-in-aid for Young Scientists (A) (No. 15681004) from the Ministry of Education, Culture, Sports, Science, and Technology.

#### References

- [1] K. P. Puntambekar, P. V. Pesavento and C. D. Frisbie, *Appl. Phys. Lett.*, **83**, 5539-5541 (2003).
- [2] O. Vatel and M. Tanimoto, *J. Appl. Phys.*, **77**, 2358-2362 (1995).
- [3] S. Ishio, T. Wasiya, H. Saito, J. Bai and W. Pei, *J. Appl. Phys.*, **99**, 093907 (2006).
- [4] M. Ishii and B. Hamilton, *Appl. Phys. Lett.*, **85**, 1610-1612 (2004).
- [5] M. Ishii, N. Rigopoulos, N. Poolton and B. Hamilton, *Physica*, **B376**, 950-954 (2006).
- [6] M. Ishii, B. Hamilton, N. R. J. Poolton, N.

Rigopoulos, S. De Gendt and K. Sakurai, *Appl. Phys. Lett.*, (in press).

[7] T. Uchihashi T, M. Ohta, Y. Sugawara, Y. Yanase, T. Sigematsu, M. Suzuki and S. Morita, *J. Vac. Sci. Technol.*, **B15**, 1543-1546 (1997).

[8] N. Sato, K. Kobayashi, S. Watanabe, T. Fujii, T. Horiuchi, H. Yamada and K. Matsushige, *Jpn. J. Appl. Phys.*, **42**, 4878-4881 (2003).

[9] M. Bowler, J. B. West, F. M. Quinn, D. M. P. Holland, B. Fell, P. A. Hatherly, I. Humphrey, W. R. Flavell and B. Hamilton, *Surf. Rev. Lett.*, **9**, 577-581 (2002).

[10] M. Ishii and B. Hamilton, *Appl. Surf. Sci.*, **248**, 14-18 (2005).

[11] C. Akita, M. Fujimoto, K. Ito, S. Shibagaki, H. Okushi, H. Haneda and J. Tanaka, *J. Appl. Phys.*, **74**, 2669-2673 (1993).

[12] Y. Obuchi, T. Kawahara, Y. Okamoto and J. Morimoto, *Jpn. J. Appl. Phys.*, **39**, 2665-2669 (2000).